

Supplementary Figure Legends

Figure S1. Histological features of periodontal aging in cynomolgus monkeys.

(A) Information of the monkeys used in this study.

(B-C) Quantitative data of hematoxylin and eosin (H&E) staining of male (B) and female (C) monkey gingival tissues. Data are shown as means \pm SEM.

(D-E) Quantitative data of Masson's trichrome staining of male (D) and female (E) monkey gingival tissues. Data are shown as means \pm SEM.

YM, young male; MM, middle-aged male; OM, old male; YF, young female; MF, middle-aged female; OF, old female. The *P*-values are indicated in the graphs, and ns indicates not significant.

Figure S2. Accumulation of aging-associated indicators in the aged primate gingiva.

(A) Immunohistochemistry staining of PCNA in gingival tissues of male monkeys. Representative images are shown on the left and quantitative data are shown as means \pm SEM on the right. Scale bars, 50 μ m.

(B-C) Immunofluorescence staining of H3K9me3 (B) and Lamin B1 (C) in gingival tissues of male monkeys. Representative images are shown on the left and quantitative data are shown as means \pm SEM on the right. Scale bars, 100 μ m and 20 μ m (zoomed-in images).

(D) SA- β -gal staining of female monkey gingival tissues (upper) and counterstaining with nuclear fast red (lower). Representative images are shown on the left and quantitative data are shown as means \pm SEM on the right. The yellow arrows indicate the SA- β -gal-positive cells. Scale bars, 200 μ m and 10 μ m (counterstaining).

(E-J) Immunohistochemistry staining of P21 (E), P-H3 (F), PCNA (G), γ -H2AX (H), LAP2 (I), and ERVW (J) in gingival tissues of female monkeys. Representative images are shown on the left and quantitative data are shown as means \pm SEM on the right. The red arrows indicate the positive cells. Scale bars, 50 μ m.

YM, young male (N=6); MM, middle-aged male (N=3); OM, old male (N=8); YF, young female (N=6); MF, middle-aged female (N=3); OF, old female (N=10). The *P*-values are indicated in the graphs and ns indicates not significant.

Figure S3. Single-nucleus transcriptomic atlas of the primate gingiva during aging.

(A) Quality control of the single-nucleus RNA sequencing data of monkey gingiva. Plots showing the \log_{10} (nucleus number), mean reads per nucleus, genome mapping rate, gene number per nucleus, unique molecular identifier (UMI) number per nucleus, and percentage of mitochondrial genes across each gingival sample of monkeys.

(B) Uniform manifold approximation and projection (UMAP) plots showing the expression profiles

of indicated cell-type-specific marker genes in monkey gingiva.

(C) Dot plots showing the expression levels of representative marker genes for each cell type.

YM, young male; MM, middle-aged male; OM, old male.

Figure S4. Aging-associated cellular and molecular characteristics of the primate gingiva.

(A) Dot plots showing the representative shared GO terms enriched for the upregulated (upper) and downregulated (lower) differentially expressed genes (DEGs) across different cell types in the monkey gingiva between different groups.

(B) Representative cell type-specific GO terms of the age-dependent upregulated (red) and downregulated (blue) DEGs in the monkey gingiva.

(C) Heatmaps showing the cell-cell interaction numbers across cell types in different aged groups of monkey gingiva.

(D) Heatmaps showing the alteration of cell-cell interaction numbers during aging across cell types of monkey gingiva.

(E) Dot plots showing the representative declined ligand-receptor pairs during aging across cell types of monkey gingiva.

YM, young male; MM, middle-aged male; OM, old male; SC, spinous cell; GC, granular cell; JE, junctional epithelium; Mito, mitotic cell; TC, T cell; BC, B cell; Macro, macrophage; EC, endothelial cell; FB, fibroblast; Peri, pericyte; Y, young; M, middle-aged; O, old.

Figure S5. The decline of YAP activity in primate gingival epithelium during aging.

(A-B) Gene set score analysis of conserved YAP signature in different epithelial cells during aging. The *P*-values are indicated in the graphs, with the blue letter representing a significant downregulation during aging, the red letter representing a significant upregulation, and the black letter representing not significant. YM, young male; MM, middle-aged male; OM, old male.

(C) Immunofluorescence staining of YAP and KRT15 in gingival tissues of female monkeys. Representative images are shown on the left and quantitative data are shown as means \pm SEM on the right. The white arrows indicate nuclear YAP-positive cells. The *P*-values are indicated in the graphs and ns indicates not significant. YF, young female (N=6); MF, middle-aged female (N=3); OF, old female (N=10). Scale bars, 100 μ m and 20 μ m (zoomed-in images).

(D) Violin plots showing the mRNA levels of *YAP* in different epithelial cells during aging. The *P*-values are indicated in the graphs, with the blue letter representing a significant downregulation during aging, the red letter representing a significant upregulation, and the black letter representing not significant.

(E) Gene set score analysis of senescence-associated secretory phenotype (SASP) and inflammatory response in basal cells during aging. The *P*-values are indicated in the graphs, with the red letter

representing a significant upregulation during aging.

Figure S6. YAP overexpression showed rejuvenation effects in human primary gingival keratinocytes

(A) The information of the healthy gingival tissue donors.

(B) Schematic diagram showing the procedure of YAP-overexpression assay in human primary gingival keratinocytes.

(C) Validation of the overexpression efficiency by Western blot. YAP protein levels are quantified as fold changes (Flag-YAP vs. Flag-Luc) and shown as means \pm SEM on the right. The *P*-value is indicated in the graph. N = 3 independent replicates.

(D) SA- β -gal staining of human primary gingival keratinocytes upon overexpression of YAP. Representative images are shown on the left. SA- β -gal positive cells are quantified as fold changes (Flag-YAP vs. Flag-Luc) and shown as means \pm SEM on the right. The *P*-value is indicated in the graph. N = 3 independent replicates. Scale bars, 200 μ m.

(E) Western blot analysis of P21 and ERVW protein expression in human primary gingival keratinocytes upon overexpression of YAP. Relative protein levels are quantified as fold changes (Flag-YAP vs. Flag-Luc) and shown as means \pm SEM on the right. The *P*-value is indicated in the graph. N = 3 independent replicates.

Supplementary Tables

Table S1. The sequence information.

Table S2. List of DEGs of bulk RNA-seq.

Table S3. List of aging-associated DEGs between different age groups of snRNA-seq.

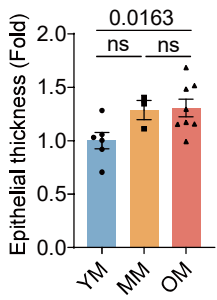
Table S4. List of ca-DEGs of snRNA-seq.

Figure S1

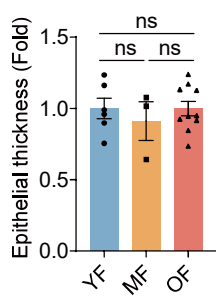
A

Male			Female		
Group	Sample number	Age (Year)	Group	Sample number	Age (Year)
Young	YM-1	5	Young	YF-1	4
	YM-2	5		YF-2	4
	YM-3	5		YF-3	4
	YM-4	5		YF-4	4
	YM-5	5		YF-5	4
	YM-6	5		YF-6	4
Middle-aged	MM-1	10	Middle-aged	MF-1	12
	MM-2	12		MF-2	11
	MM-3	11		MF-3	11
Old	OM-1	18	Old	OF-1	17
	OM-2	17		OF-2	16
	OM-3	16		OF-3	17
	OM-4	18		OF-4	16
	OM-5	18		OF-5	19
	OM-6	16		OF-6	16
	OM-7	17		OF-7	18
	OM-8	16		OF-8	18
			OF-9	18	
			OF-10	17	

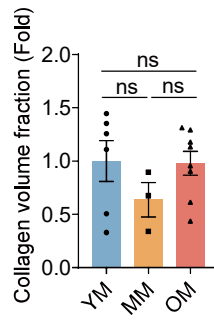
B



C



D



E

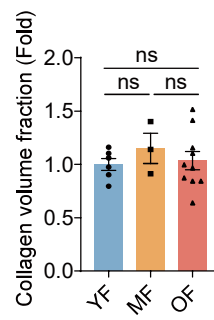


Figure S2

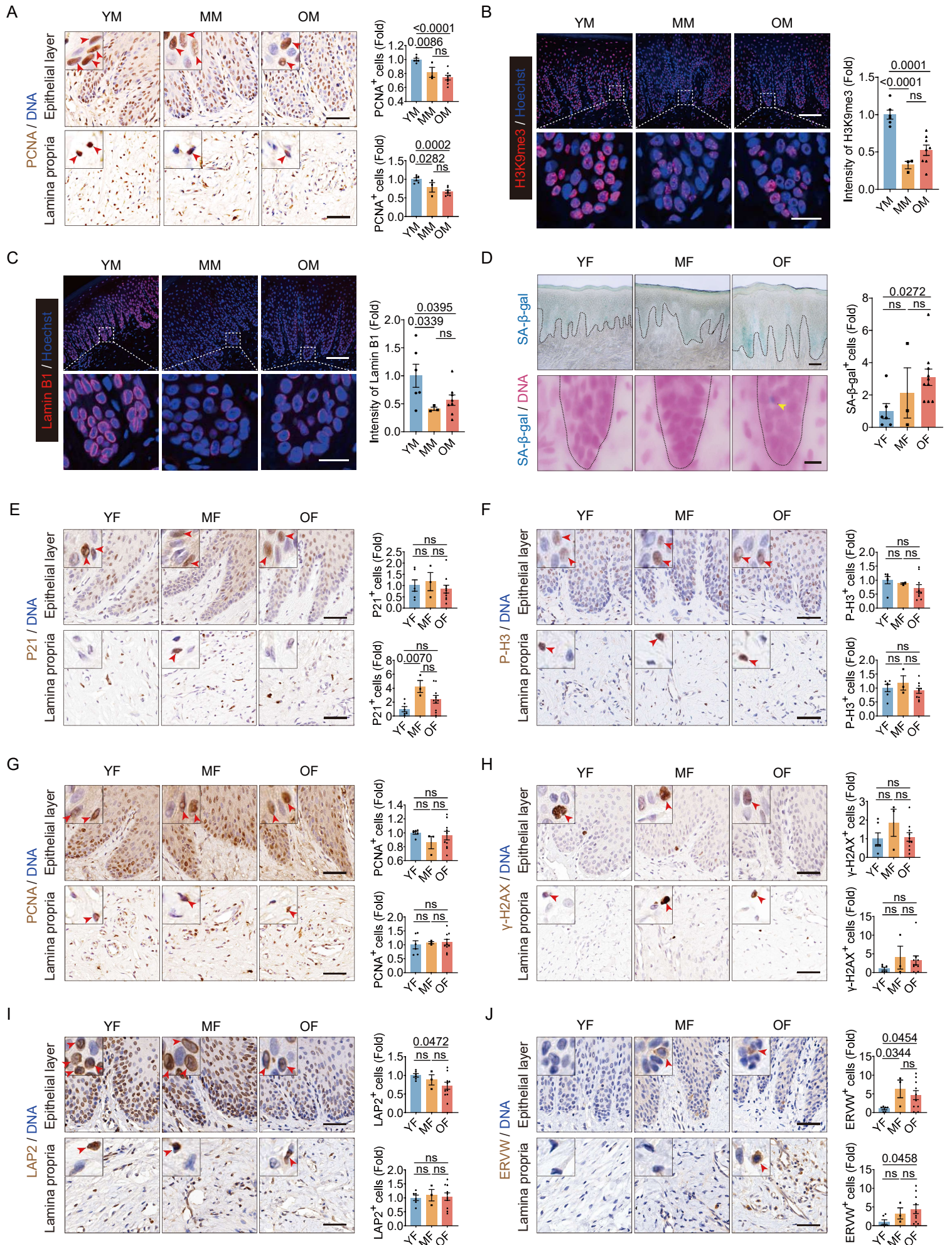
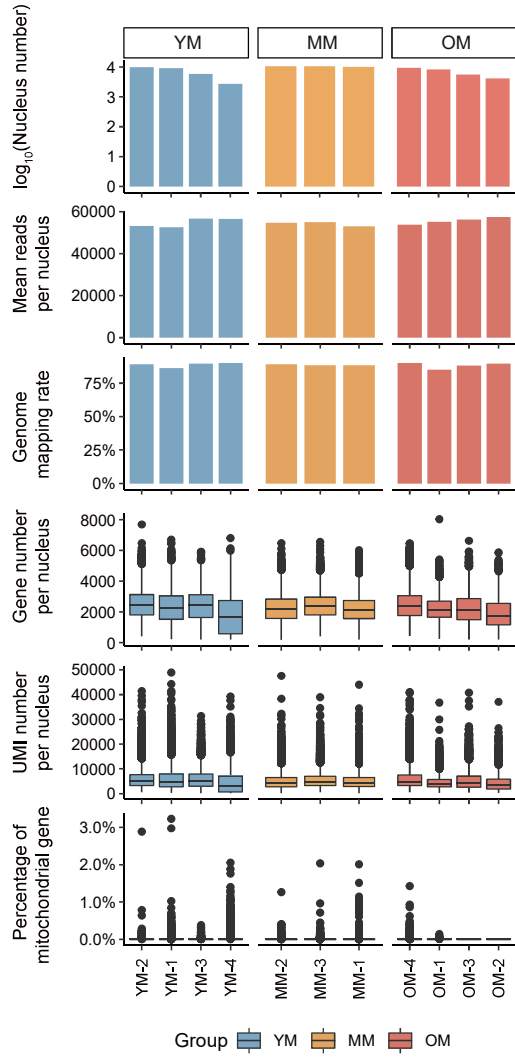
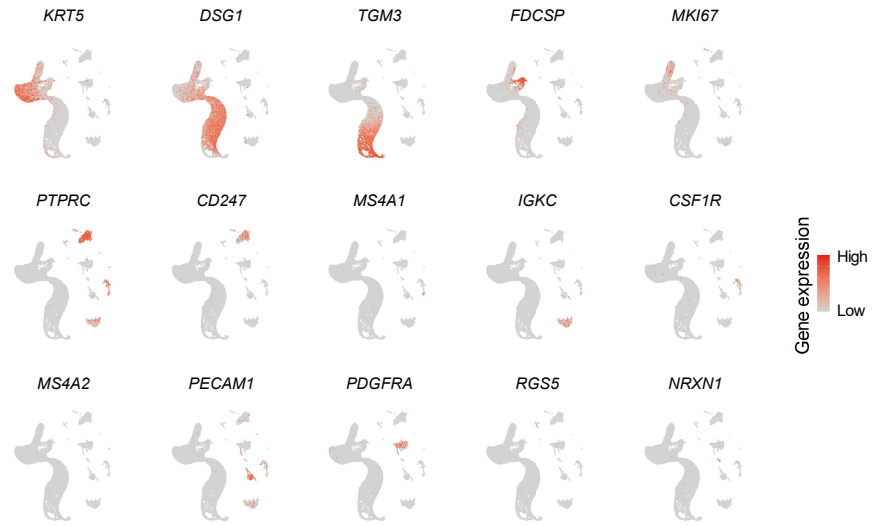


Figure S3

A



B



C

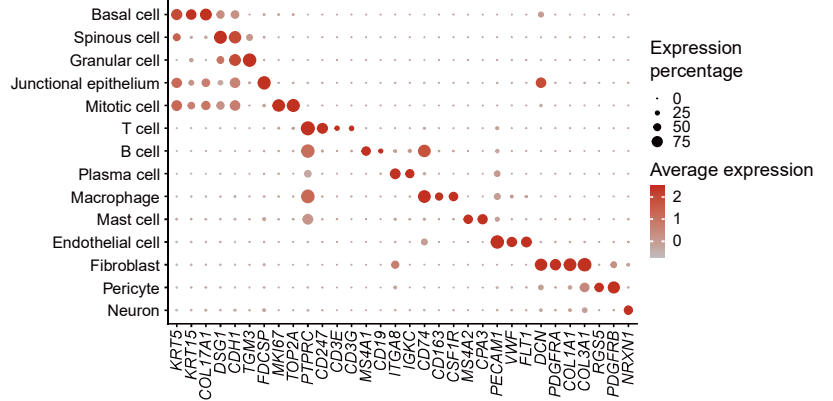
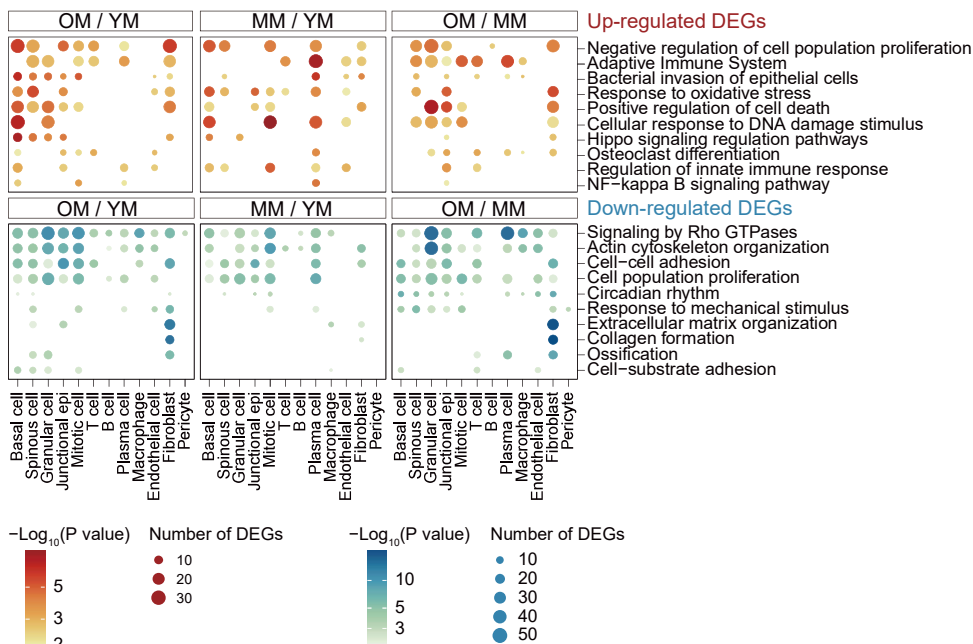
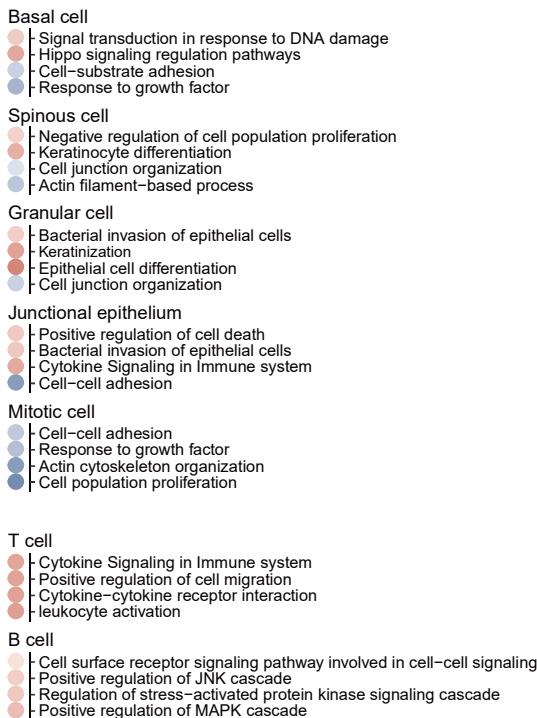


Figure S4

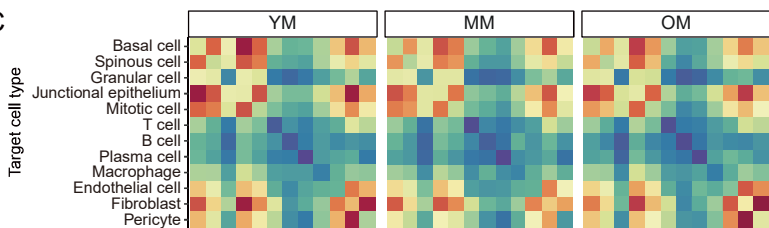
A



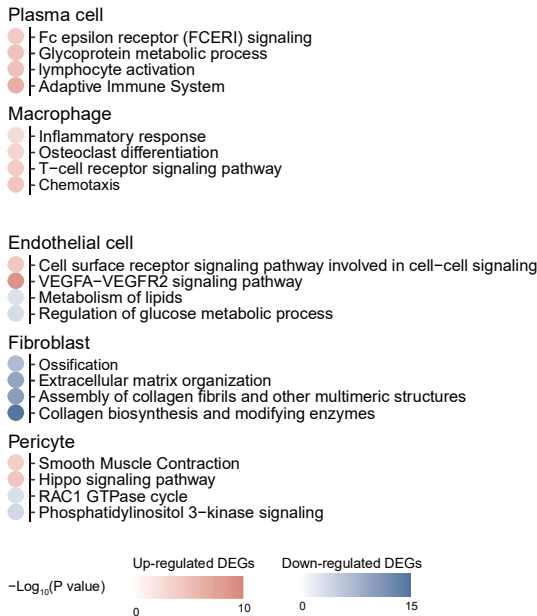
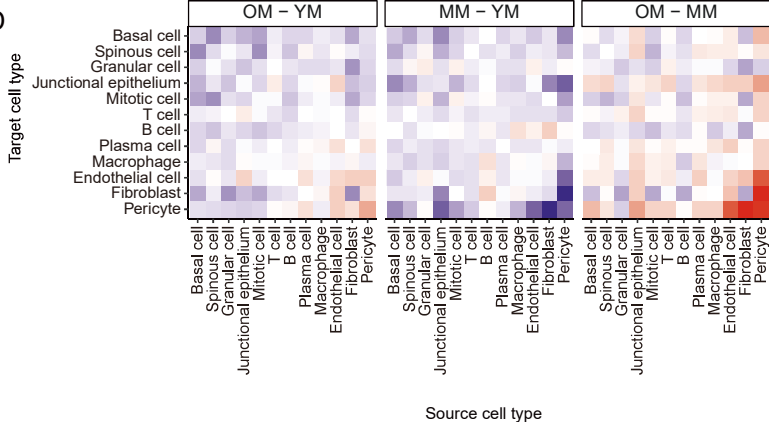
B



C



D



E

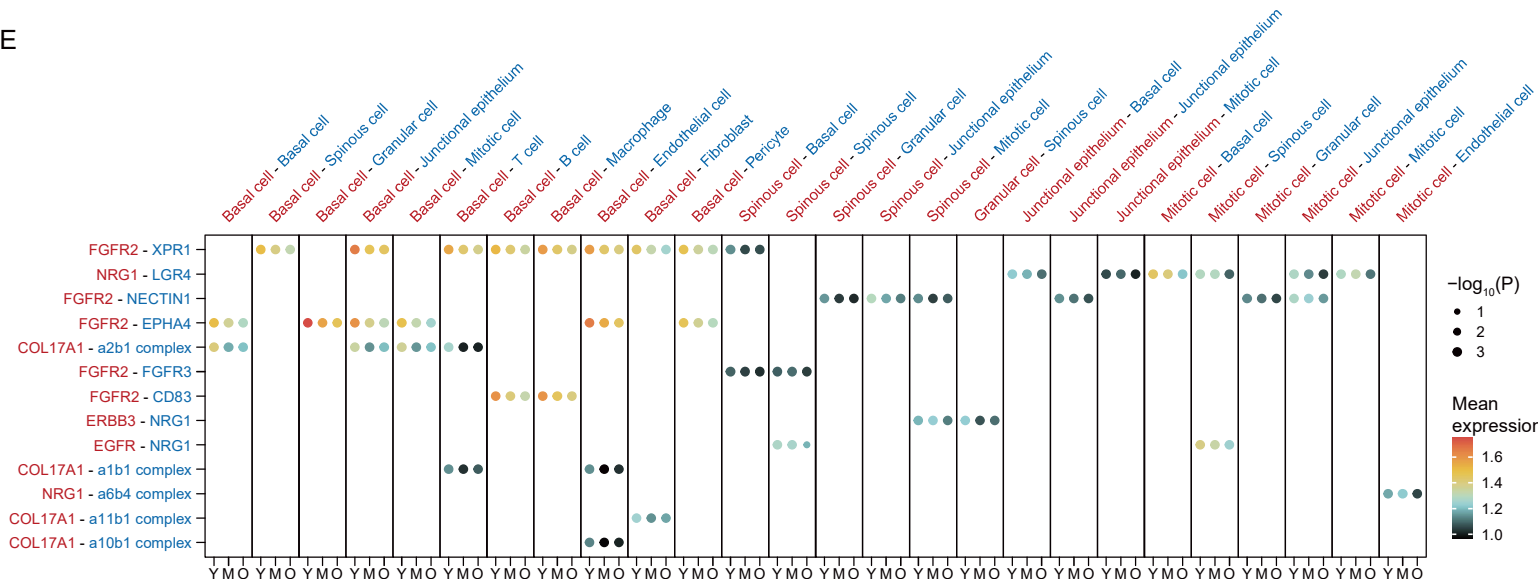


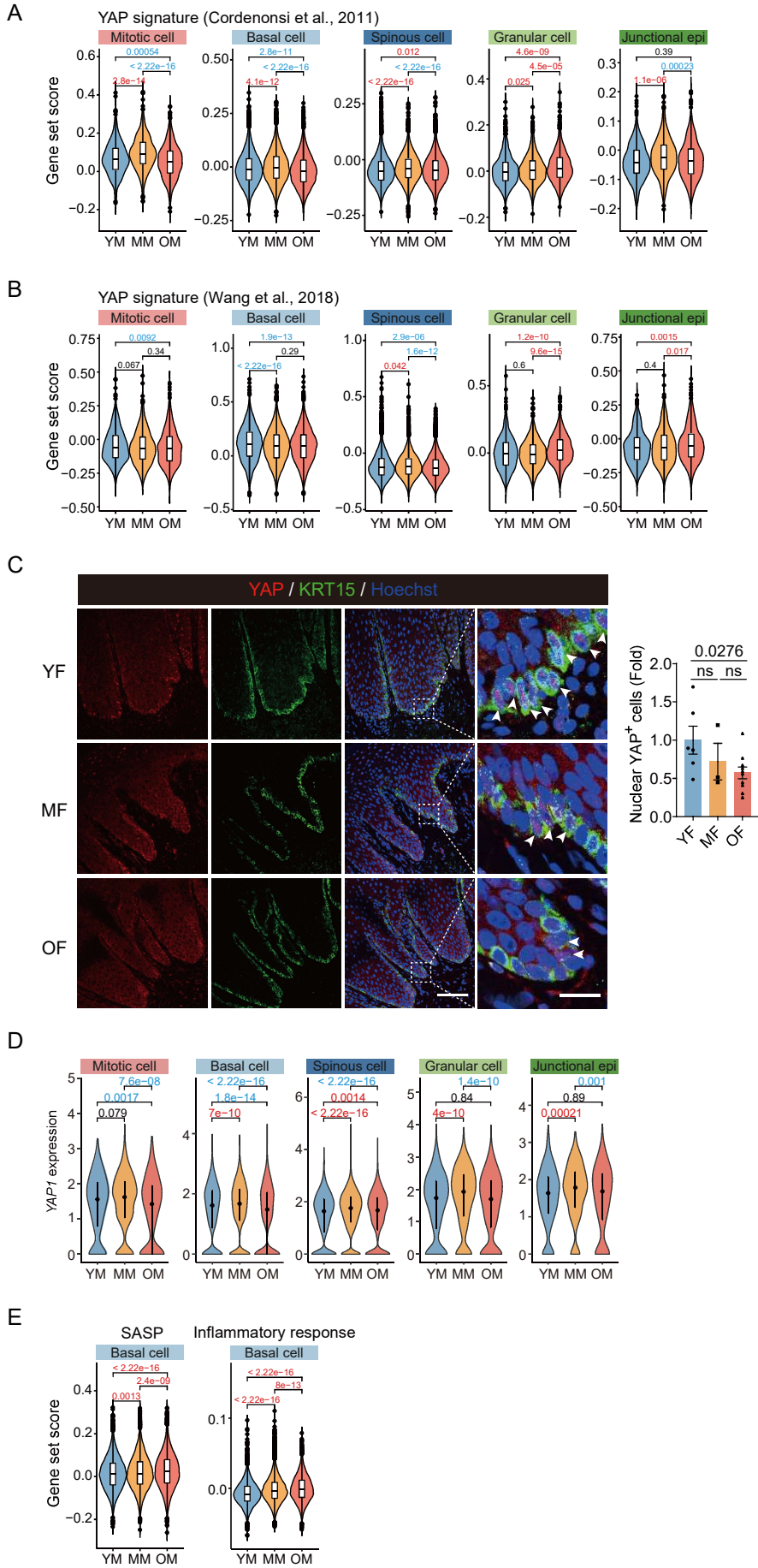
Figure S5

Figure S6

A

No.	Sex	Age (Year)
1	Female	14
2	Female	16
3	Female	21
4	Male	24
5	Male	24
6	Male	26
7	Male	26
8	Female	26
9	Male	27
10	Female	27
11	Female	29
12	Female	37
13	Male	39
14	Female	40
15	Male	46
16	Male	53
17	Male	58
18	Male	70

